Chem. Senses 26: 385–398, 2001

# Fluid Dynamic Design of Lobster Olfactory Organs: High Speed Kinematic Analysis of Antennule Flicking by *Panulirus argus*

**J.A. Goldman and M.A.R. Koehl**

Department of Integrative Biology, University of California, Berkeley, CA 94720-3140, USA

*Correspondence to be sent to: J. Goldman, Department of Biology, Duke University, Box 90338, Durham, NC 27708-0338, USA. e-mail: jag14@duke.edu*

## Abstract

Many organisms use olfactory appendages bearing arrays of microscopic hairs to pick up chemical signals from the surrounding water or air. We report a morphometric and high speed kinematic analysis of the olfactory organs (lateral flagella of the antennules, which bear chemosensory aesthetasc hairs) of the spiny lobster, *Panulirus argus*. *Panulirus argus* sample specific locations by executing a rapid series of antennule flicks at one position, moving the antennule to a different spot and then performing another series of flicks. Odorant delivery to an aesthetasc depends on the water motion near it, which depends on its Reynolds number (Re, proportional to both the diameter and speed of the hair). High speed video enabled us to resolve that during a series of flicks, an antennule moves down rapidly (aesthetasc Re = 2) and up more slowly (Re = 0.5), pausing briefly (~0.54 s) before the next downstroke. The antennules of *P. argus* operate in a range of Re values and inter-aesthetasc spacings in which penetration of fluid between the hairs in an array is especially sensitive to changes in speed. Therefore, when antennules flick 'old' water is flushed out of the aesthetasc array during the leaky downstroke and is not picked up again during the less leaky upstroke, hence the antennules can take discrete samples. Thus, by operating in this critical Re range these antennules should be particularly effective at sniffing.

## Introduction

A critical step in the process of olfaction is the arrival of chemical signals from the environment to the surface of a chemosensory structure. From a hydrodynamic standpoint this process can be broken up into two regimes based on scale: (i) large-scale turbulent water flow transports the odorant plume from the source to the immediate vicinity of the sensor; (ii) small-scale viscous flow and molecular diffusion govern the transport of the odorant to the surface of the sensor (DeSimone, 1981; Koehl, 1996). The first step in filtering the spatial and temporal information contained in odor plumes (Murlis, 1986; Weissburg and Zimmer-Faust, 1994; Willis *et al*., 1994; Atema, 1995) depends on the physical manner in which an olfactory structure affects fluid flow across its surfaces (Moore *et al.*, 1989; Atema, 1995; Koehl, 1996, 2000a).

### Fluid flow around arrays of sensory hairs at low Reynolds number

Many organisms use appendages bearing arrays of microscopic hair-like sensilla to pick up chemical signals from the surrounding water or air. When a fluid moves past the surface of a structure, such as a sensory hair, the layer of fluid in contact with the surface does not slip relative to it, hence a velocity gradient develops in the fluid between the structure and the mainstream flow. The thickness of this velocity gradient depends on the Reynolds number (Re), which represents the relative importance of inertial to viscous forces for a particular flow situation:

$$\mathrm{Re} = LU\rho/\mu$$

where $L$ is a length scale such as hair diameter, $U$ is fluid velocity relative to the hair and $\rho$ and $\mu$ are fluid density and viscosity, respectively. By convention, when calculating the Re of a cylinder in an array of cylinders, such as a fiber in a fibrous filter, the diameter of the cylinder is used for $L$ and the free stream velocity arriving at the array is used for $U$ (Fuchs, 1964; Davies, 1973; Rubenstein and Koehl, 1977; Shimeta and Jumars, 1991). The Re values of olfactory sensilla of a variety of arthropods are low: $10^{-4}$–10 (Loudon *et al.*, 1994; Mead *et al.*, 1999). Although inertial effects cannot be ignored at the upper end of this Re range, the viscous flow near these sensory hairs is laminar [i.e. fluid motion is smooth and orderly, with no random fluctuations in velocity (Happel and Brenner, 1965; Vogel, 1994)]. At these low Re values laminar velocity gradients are thick relative to the dimensions of a hair (Cheer and Koehl, 1987a). Since there is no turbulent mixing in a laminar

velocity gradient, molecular diffusion alone moves odorants across stream lines towards or away from the sensillum surface.

Theoretical analyses (Cheer and Koehl, 1987a,b; Koehl, 1992, 1995, 1996) and model experiments (Hansen and Tiselius, 1992; Koehl, 1992, 1996, 2000a; Leonard, 1992; Loudon *et al*., 1994) of flow around and through various arrays of cylinders have elucidated how the steepness of velocity gradients adjacent to the cylinders and the leakiness of the array to fluid movement between neighboring cylinders depends on cylinder speed, diameter, spacing, length and motion relative to nearby body surfaces. 'Leakiness', defined in Cheer and Koehl (Cheer and Koehl, 1987a), is a measure of the proportion of the fluid encountered by an array of cylinders that flows through it rather than around it. Leakiness equals the volume of fluid per time that flows through the gap between neighboring cylinders divided by the volume of fluid per time that would flow through a space of the same size if the hairs were not present. Although the mathematical model of Cheer and Koehl (Cheer and Koehl, 1987a) calculates flow between a pair of cylinders perpendicular to the flow, the velocities and leakinesses predicted by that model for animal appendages bearing complex arrays of hairs at various orientations (e.g. antennae of moths, cephalic fans of black flylarvae and second maxillae of copepods) match measurements of flow through the real appendages (Koehl and Cheer, 1987b; Koehl, 1995). Therefore, the general principles about flow through arrays of cylinders provided by such simple models can provide insights about the function of arrays of hair-like olfactory sensilla.

The mathematical and physical models cited above reveal a transition in the fluid dynamic performance of arrays of hairs: at low Re values fluid flows around rather than through arrays of hairs, whereas at higher Re values fluid readily moves between neighboring hairs and hair-bearing appendages are quite leaky. The hair Re range in which the transition from non-leaky to leaky behavior occurs depends on the spacing of the hairs (Koehl, 1995, 2000a); the more closely spaced the hairs, the higher the Re range in which the leakiness of the array is affected by changes in Re (i.e. changes in velocity). For arrays of closely spaced hairs (i.e. arrays in which the width of gaps between hairs is ≤5 hair diameters) the leakiness of the array is especially sensitive to changes in velocity in the hair Re range $10^{-1}$–10. Therefore, determining how an olfactory appendage functions depends on knowing the Re range in which its hairs operate.

### Fluid flow near sensilla and odorant stimulation of neurons

Odor plumes in turbulent ambient flow are filamentous [see figure 5 in Koehl (Koehl, 2000a)] and it has been suggested that the heterogeneity in concentration in a plume can provide information about distance from the odor source (Moore and Atema, 1988, 1991; Zimmer-Faust *et al.*, 1988; Moore *et al.*, 1994; Atema, 1996). Indeed, the concentration and the rate of change of concentration of odorant arriving at olfactory neurons can affect their response. For example, Gomez and Atema pulsed odorant onto exposed axons of lobster olfactory receptor neurons and found that both higher concentrations of odorant and longer pulses of application increased the number of spikes produced by a cell (Gomez and Atema, 1996). Higher concentration also reduced the delay between odorant application and the first spike. Moore's mathematical model of adaptation and disadaptation in olfactory receptor neurons suggested that a population of cells with different rates of adaptation can distinguish between different rates of concentration increase at the onset of an odor pulse (Moore, 1994).

The small-scale fluid flow around an olfactory sensillum containing sensory neurons affects the rates and numbers of odorant molecules arriving at the surface of the sensillum. A row of hairs with low leakiness does not process fluid rapidly, but low fluid velocity between neighboring hairs allows a long time for molecules to diffuse onto the hairs and thus a large proportion of the molecules in the fluid may be caught (Murray, 1977; Rubenstein and Koehl, 1977; Shimeta and Jumars, 1991). However, a theoretical analysis by Koehl indicated that if an array of hairs is moved more rapidly: (i) the volume flow rate through it rises, increasing molecule encounter rates even though a smaller proportion of the odorants passing through the array have time to diffuse to hair surfaces; (ii) velocity gradients along hair surfaces become steeper, increasing sensitivity to changes in odorant concentration (Koehl, 1996).

Although the measurements that have been made of the leakiness of arrays of hairs on arthropod appendages are consistent with the predictions of our models (Koehl and Strickler, 1981; Vogel, 1983; Cheer and Koehl, 1987b; Koehl, 1996), how the structure of and flow speed past hair-bearing olfactory appendages affect molecule capture needs to be tested for diverse animal antennae. The first step in any such analysis is to quantify the morphology of the antenna and the water or air motion relative to it and, in particular, to determine the Re range in which the sensilla on the appendage operate. Therefore, the present study has measured the morphology and kinematics of the olfactory antennules of the Florida spiny lobster, *Panulirus argus*, and determined the Re of the sensilla on those antennules, the hair-like aesthetascs.

### Antennule flicking by lobsters

The lateral branches (flagella) of the antennules of decapod crustaceans bear tufts of hairs in a great variety of arrangements (Laverack, 1988) and the aesthetasc hairs they bear serve an olfactory function [evidence reviewed by Atema, Gleeson, Grunert and Ache, Hallberg *et al.* and Atema and Voigt (Atema, 1977, 1995; Gleeson, 1982; Grunert and Ache, 1988; Hallberg *et al.*, 1992; Atema and Voigt, 1995)]. Decapod lateral antennules have been used as

model systems for studying the electrophysiology of olfactory neurons [reviewed by Ache, Atema and Atema and Voigt (Ache, 1982, 1988; Atema, 1985; Atema and Voigt, 1995)]; among the most extensively studied model species has been the lobster *P. argus* (Fuzessery *et al*., 1978; Schmidt and Ache, 1979; Bayer *et al*., 1980; Anderson and Ache, 1985; Marscall and Ache, 1989; Michel *et al*., 1991). The distal portion of the lateral branch of an antennule of *P. argus* bears rows of aesthetascs flanked by larger guard hairs (Grunert and Ache, 1988; Gleeson *et al*., 1993) (Figure 1). Ultrastructural studies (Grunert and Ache, 1988) showed that each *P. argus* aesthetasc contains several hundred chemoreceptor cells.

A variety of crustaceans flick their olfactory antennules. Schmidt and Ache, Gleeson and Atema (Schmidt and Ache, 1979; Gleeson, 1982; Atema, 1985) suggested that closely spaced hairs on the antennules of various crustaceans inhibit water flow and odor access. Microelectrode measurements by Moore *et al*. (Moore *et al*., 1989, 1991) of reduced fluxes of tracer molecules within aesthetasc tufts on the lateral flagella of the antennules of the clawed lobster, *Homarus americanus*, but not near their smooth medial flagella, corroborated this suggestion. Antennule flicking has been described as a mechanism of reducing velocity gradient thickness, thereby increasing access of odors to receptor cells (Schmidt and Ache, 1979; Atema, 1985). Several lines of evidence are consistent with this idea. Flow pulses onto the aesthetascs of antennule preparations (meant to mimic flicking) increased penetration of tracer molecules into aesthetasc tufts of *H. americanus* (Moore *et al*., 1989, 1991) and of dye into aesthetasc arrays of *P. argus* (Gleeson *et al*., 1993) and enhanced the response of *P. argus* olfactory receptor neurons to changes in odor concentration (Schmidt and Ache, 1979).

Although such experiments with antennule preparations reveal the importance of water motion to antennule reception of chemical signals, they cannot provide quantitative information about the effects of antennule flicking on the filtering of odorant signals unless they mimic the water flow relative to the aesthetascs during the course of a flick. Although video records of *P. argus* flicking have been made (Gleeson *et al*., 1993), the framing rate of standard video (typically 30 frames/s) is not fast enough to capture the details of antennule position, shape and orientation during this brief motion. Therefore, the present study has used high speed video analysis to quantify the kinematics of lateral antennule flicking by *P. argus*, providing the data necessary so that future neurobiological experiments using antennule preparations can be designed to have biologically relevant odorant delivery.

In addition, we provide values for the morphometric and kinematic parameters necessary to develop mathematical and physical models of *P. argus* antennules. Such models permit measurement of the details (which are unmeasureable on real flicking antennules) of the velocity gradients around and through arrays of aesthetascs. Such models also enable us to manipulate the design of the antennules (in ways not possible in experiments with living lobsters) to assess how morphological and kinematic parameters influence antennule performance. Although some morphological information for *P. argus* is available in the literature (Grunert and Ache, 1988; Gleeson *et al*., 1993), a number of fluid dynamically important parameters required for model development have not yet been measured.

## Materials and methods

### Animals

*Panulirus argus* from Florida were kept in a 246 l aquarium filled with artificial seawater (Instant Ocean) at 25°C. Clay flower pots and rocks provided refuges for the lobsters. We focused on animals within a narrow range of intermediate body size (0.06–0.08 m carapace length), thereby minimizing variation that might be introduced by possible differences in the chemosensory ecology of very small or very large animals (Marx and Herrnkind, 1985; Ratchford and Eggleston, 1998; Mead *et al*., 1999).

Each lobster was fed one dead raw shrimp (~50–150 g) every other day. Shrimps were stored in a freezer. Each shrimp was thawed under tap water and shelled immediately before presenting it to the lobsters. Each food item was presented to the lobsters by placing it haphazardly in the tank. Lobsters were able to find the food item quickly and usually began to eat immediately thereafter. The purpose of this feeding regime was not to mimic the varied natural diet of the lobsters, but rather to condition them to a predictable type of food before videotaping their antennule flicking in response to food.

### Kinematics

The kinematics of flicks by the lateral flagella of the antennules of *P. argus* were measured from high speed video records made at 250 frames/s using a Kodak Ektapro TR High Speed Video System with an intensified imager. Lobsters were placed in a small aquarium (0.20 × 0.32 × 0.20 m) containing still artificial seawater at 25°C. We filmed the lobsters in small aquaria to increase the probability that they would flick an antennule in the field of view and focal plane of the camera. The still water condition under which we videotaped the lobsters is biologically relevant because *P. argus* live in dens in rock outcrops or in aggregations of stony corals, soft corals or sponges (Kanciruk, 1980); field measurements of water flow within aggregations of corals reveal very slowly moving water, even when ambient currents and waves at the sites are fast (Koehl and Hadfield, 1999). We began videotaping when lobsters stood still with the lateral flagellum of one antennule flicking in a plane parallel to the camera lens. We analyzed the downstroke and upstroke of the first 15 flicks after taping began.

We analyzed the kinematics of antennule flicking using a

Peak Performance Motion Analysis System (Peak Performance Technologies, v.5.0). Our high speed video provided a temporal resolution of 0.004 s per frame; using this high framing rate we were able to record clear images of an antennule that were not blurred by the motion of the antennule during a frame. Although the high framing rate was necessary to obtain clear images of the position of the lateral flagellum with a temporal resolution of 0.004 s, the distance moved by the antennule in the short interval between frames was very small. Thus, we digitized the antennule on every tenth frame to ensure that the distance it moved was large relative to the pixel size of the screen. By sampling frames at different time intervals we found that 0.04 s was the shortest interval to yield repeatable measurements of the distance traveled by the lateral flagellum of the antennule. Therefore, we digitized by hand the tip of the lateral flagellum of an antennule and the mid-point of the region of the flagellum bearing the tuft of aesthetascs at 0.04 s intervals to calculate their velocities. We estimated our digitizing error by redigitizing the same video sequences on three separate days; the measurements of velocity were repeatable to the nearest 0.01 m/s.

We measured the instantaneous angle of attack of each antennule lateral flagellum (the angle between the long axis of the flagellum at some position along its length and the velocity vector of water motion relative to the flagellum) during each flick. For example, the angle of attack of the lateral flagellum at the mid-point of its tuft of hairs was calculated as the angle between the instantaneous trajectory of that position on the flagellum and its instantaneous long axis. Since we videotaped at a rate of 250 frames/s, each image we used to define 'instantaneous' flagellum orientation averaged the antennule over a period of 0.004 s (see Figure 4B–D).

In summary, a temporal resolution of 0.004 s was necessary to resolve the instantaneous position and orientation of the lateral flagellum, whereas the most repeatable measurements of velocity were obtained by sampling these high speed videos at 0.04 s intervals.

### Temporal and spatial pattern of flicking

Video records of lobsters in the large aquarium were made using a Sony Hi-8 CCD-TR101 camcorder. No shrimp had been added to the aquarium for at least 24 h prior to the videotaping and ~30% of the water in the aquarium had been replaced by new artificial seawater 2 h prior to videotaping. We videotaped undisturbed lobsters before, during and after food (dead shrimp, as described above) was dropped into the aquarium. These videos were analyzed using a JVC HR-S6600U VCR to record the time (to the nearest 0.033 s) and vertical position (measured with a ruler to the nearest 5 mm) of the tip of the lateral flagellum of an antennule at the onset of each flick.

### Morphometrics

We removed the lateral flagellum of either the left or right antennule of each *P. argus* after it had been videotaped and immediately fixed each antennule in 1% glutaraldehyde in artificial seawater buffered at pH 7.4 with 0.2 M cacodylate. After rinsing with seawater, the middle section of the region of the antennule bearing sensory hairs was isolated and cut into three pieces. Guard hairs were removed from the distal third, guard hairs and aesthetascs were removed from the middle third and all hairs were left intact on the proximal third. These antennule pieces were dehydrated in an ethanol series, dried in a critical point drier (Samdri PVT-3B; Tousimis Research Corp.), mounted on SEM stubs and coated with gold to a thickness of 25 nm (Polaron E-5400 sputter coater). Specimens were viewed in an ISI DS-130 scanning electron microscope and micrographs were taken of undamaged sections of the antennules. The first three distal-most segments in each micrograph were digitized (Jandel Scientific digitizing pad, Sigma Scan software v.3.01) to obtain measurements for guard hair angle (b) and diameter (a), aesthetasc length (c) and diameter (d), distance between (e, f) and width (g) of aesthetasc rows, spacing of guard hairs (k) and asymmetric sensilla (j, h) with respect to aesthetascs and number of aesthetascs per row (i) (Figure 1).

The spacing and orientation of the rows of aesthetascs were measured using video images of antennules taken through a Wild Heerbrugg M5A stereomicroscope with a Watac WAC-902 video camera and Panasonic AG-6300 VCR. We removed the guard hairs from the region of the antennule just proximal to the mid-section that was used for SEM and captured video images of the antennule in three orientations: (i) aesthetasc tips pointing towards the camera; (ii) aesthetascs parallel to the camera lens with the medial hairs uppermost; (iii) aesthetascs parallel to the camera lens with the lateral hairs uppermost. The following parameters were digitized (as described above) using tracings on transparencies of video images of the three distal segments of the specimen: angles of the rows formed by the aesthetasc tips (o, p, q); width of the aesthetasc row at the tips (l); distances between the tips of the lateral-most aesthetascs in neighboring rows (n); distances between the tips of the medial-most aesthetascs in neighboring rows (m); angles of the aesthetascs to the axis of the flagellum of the antennule (r, s, t, u) (Figure 1).

Repeated measurements of the same features were made on three separate days for both the SEM micrographs and the light microscope video images. We found that the measurements of angles were repeatable to the nearest 1° and that measurements of linear dimensions had two significant figures.

### Calculation of aesthetasc Reynolds number

The Reynolds numbers of the aesthetascs during the flick

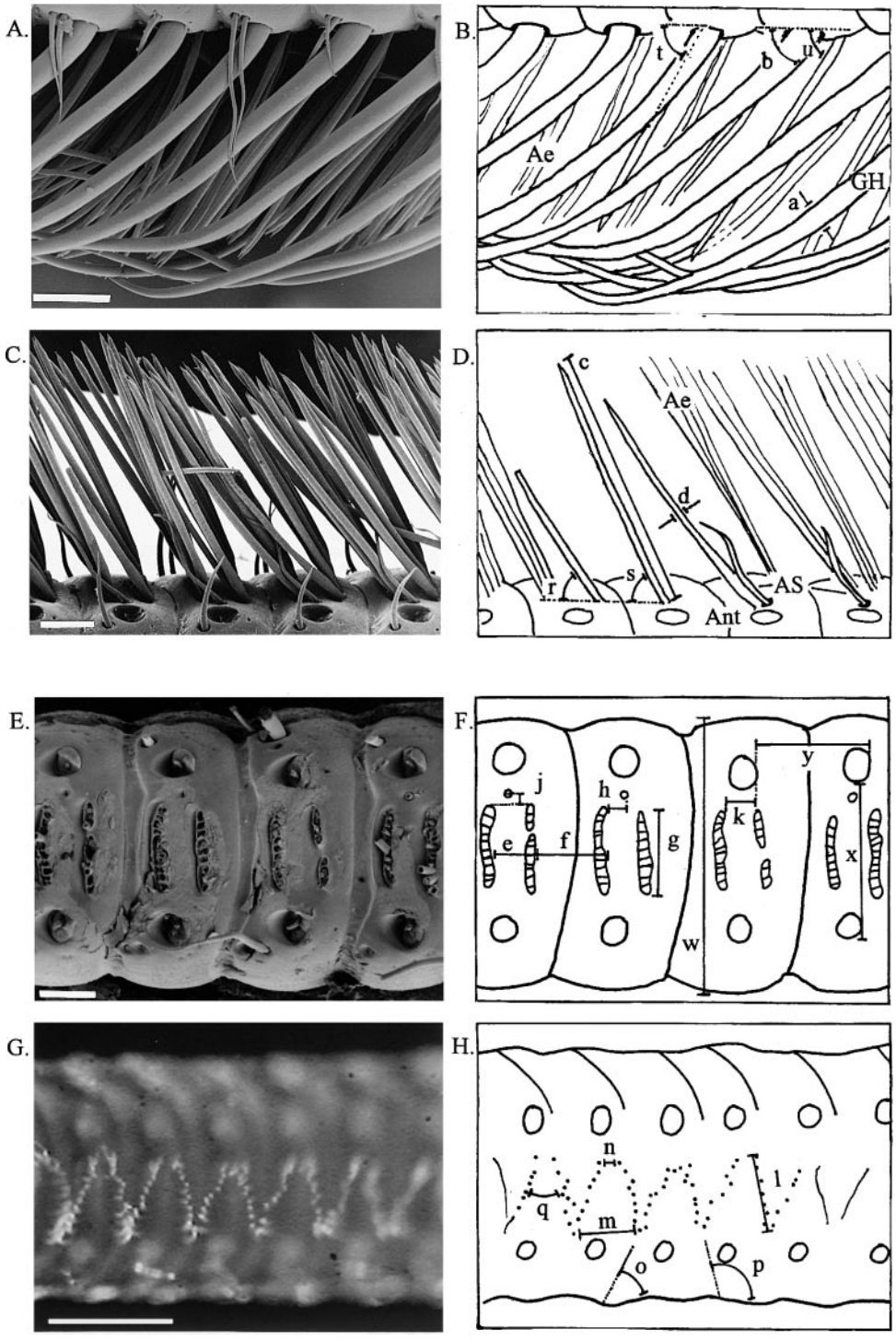


**Figure 1** Morphological parameters of the hair-bearing region of the lateral branch of antennules of *P. argus*. w, width of lateral branch of antennule; x, distance between guard hairs along one segment; y, distance between guard hairs on adjacent segments; Ant, antennule; GH, guard hair; Ae, aesthetasc; AS, asymmetric sensillum. All other code letters defined in Table 1. The hairs of the lateral branch of antennules project ventrolaterally. In all pictures the distal end of the antennule is to the left. **(A)** SEM of the medial-most portion of a right antennule, showing the guard hairs and aesthetascs. Scale bar 200 μm. **(B)** Tracing of the SEM in (A) showing morphological parameters measured. **(C)** SEM of the lateral-most side of a right antennule from which the guard hairs have been removed to show the aesthetascs and asymmetric sensilla. Scale bar 150 μm. **(D)** Tracing of the SEM in (C) showing morphological parameters measured. **(E)** SEM of a ventrolateral view of a left antennule from which the guard hairs, aesthetascs and asymmetric sensilla have been removed. Scale bar 150 μm. **(F)** Tracing of the SEM in (E) showing morphological parameters measured. **(G)** Light micrograph of a ventrolateral view of a left antennule from which the guard hairs have been removed. Only the tips of the aesthetascs are in the plane of focus. Scale bar 500 μm. **(H)** Tracing of the micrograph in (G) showing morphological parameters measured.

downstrokes and upstrokes were calculated for each lobster. Re = $LU\rho/\mu$, where $L$ is aesthetasc diameter measured for each animal, $U$ is mean speed of the mid-point of the hair tuft on the antennule measured for each animal, $\rho$ is the density of seawater at 25°C = 1023 kg/m$^3$ (Zerbe and Taylor, 1953) and $\mu$ is the viscosity of seawater at 25°C = $9.6 \times 10^{-4}$ Pa s (Sverdrup *et al.*, 1942). Since the aesthetascs do not move relative to the lateral flagellum to which they are attached, we assumed that the velocity of the aesthetascs through the water was the same as the velocity of the lateral flagellum. Therefore, we assumed that the free stream water velocity relative to the array of aesthetascs was equal in magnitude (i.e. speed) and opposite in direction to the velocity of the lateral flagellum. As described in the Introduction, the local flow velocity in the immediate vicinity of a small hair in the middle of an array of hairs can be much lower than free stream. However, the free stream velocity relative to the array is, by convention, used to calculate the Re of the cylinders in the array. Knowing the aesthetasc Re and the width of the gaps between the cylinders, one can then use the results of Cheer and Koehl (Cheer and Koehl, 1987a) to estimate the leakiness (defined in the Introduction) of the array of hairs.

### Orientation of aesthetascs during a flick

During a flick the direction of water flow relative to the antennule is parallel, but in the opposite direction, to the motion of the antennule. We measured the angle of the tuft of hairs on the lateral flagella of antennules with respect to the water flow past the flagella during a flick (v) (Figure 2) from video records of the tips of antennules. We clamped antennules that had been removed from lobsters such that the long axis of the lateral flagellum was perpendicular to the lens of a video camera (Sony Hi-8 CCD-TR101). The joint at the base of the lateral flagellum only permits the flagellum to move in one plane relative to the base, hence we could manually push on the proximal end of the lateral flagellum to simulate the orientation of a flick. We digitized the angle between the trajectory of the flick and the tuft of hairs on the flagellum to the nearest 1°, as described above. We assumed that the angle of the aesthetascs during a natural flick by *P. argus* is the same as the angle we measured by this technique because we observed that the aesthetascs did not bend or reorient relative to the lateral flagellum when we streamed water currents across antennules or manually flicked them at realistic velocities.

### Statistics

Student's *t*-tests were performed as described by Zar (Zar, 1974) and all other statistical analyses were conducted using Systat software v.5.04.

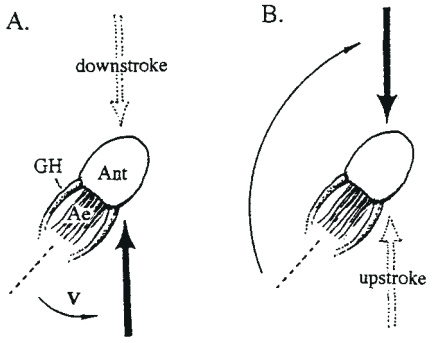


**Figure 2** Diagram of a cross-section of a lateral branch of a right antennule (as viewed from its distal end) of *P. argus* showing the orientation of the aesthetascs with respect to the direction of antennule flicking. The direction of antennule motion is indicated by the dotted arrow and the direction of water motion relative to the antennule is indicated by the solid arrow. Ant, lateral flagellum of antennule; Ae, aesthetascs; GH, guard hair. **(A)** During the downstroke (angle v is defined in Table 1). **(B)** During the upstroke.

## Results

### Morphology

The basic morphology of the hair-bearing region of the lateral flagellum of the antennule of a *P. argus* is illustrated in Figure 1. We measured a zig-zag arrangement of the tips of the aesthetascs (Table 1), as reported by Grunert and Ache and Gleeson *et al.* (Grunert and Ache, 1988; Gleeson *et al.*, 1993). Like Gleeson *et al.*, we also observed that the aesthetascs did not point directly into the flow during the flick downstroke, but rather were at an acute angle (v = 32 ± 4°, $n$ = 3) with respect to the flow on the downstroke and at an obtuse angle (148°) with respect to the flow during the upstroke (Figure 2).

Our morphometric data for the lateral flagella of the antennules of *P. argus* are reported in Table 1. None of the morphological parameters listed in Table 1 varied significantly with carapace length (linear regression, slopes not significantly different from 0, $P > 0.05$ in all cases), suggesting that aesthetasc size, spacing and orientation, as well numbers of aesthetascs and guard hairs per segment, were maintained across the range of body sizes we studied. Gleeson *et al.* also found no significant differences in aesthetasc morphology between the three lobsters they measured (carapace lengths 0.058–0.076 m) (Gleeson *et al.*, 1993). Although the diameter of the guard hairs did not change significantly across the animal size range we studied, the width of the lateral flagellum of the antennule did increase significantly with body size (Figure 3A), as did the spacing between guard hairs (Figure 3B,C). Guard hair spacing and antennule width appeared to scale geometrically (Alexander, 1971) across the size range of *P. argus* studied (the slopes of linear regressions of log-log plots of antennule width and of guard hair spacing versus carapace length were not significantly different from 1, Student's *t*-test, $P > 0.05$ in all cases).

**Table 1** Morphological parameters of the lateral antennule of the lobster, *P. argus*

| Code | Morphological feature (units) | Mean ± SD | *n* | *s* |
|---|---|---|---|---|
| a | Guard hair diameter (28μm) | 60 ± 9 | 7 | 3 |
| b | Guard hair angle (°) | 39 ± 4 | 7 | 3 |
| c | Aesthetasc length[a] (28μm) | 720 ± 50 | 7 | 6 |
| d | Aesthetasc diameter[a] (28μm) | 22 ± 3 | 7 | 6 |
| e | Distance between aesthetasc rows on same segment (28μm) | 110 ± 10 | 7 | 3 |
| f | Distance between aesthetasc rows on adjacent segments (28μm) | 170 ± 20 | 7 | 3 |
| g | Width of aesthetasc row at base[a] (28μm) | 230 ± 20 | 7 | 6 |
| k | Distance between aesthetasc row and guard hair (28μm) | 60 ± 10 | 7 | 3 |
| i | Number of aesthetascs per row[a] | 10 ± 1 | 7 | 6 |
| j | Distance laterally of asymmetric sensillum from aesthetascs (28μm) | 31 ± 6 | 7 | 3 |
| h | Distance proximally of asymmetric sensillum from aesthetascs (28μm) | 40 ± 10 | 7 | 3 |
| l | Width of aesthetasc row at tips[a] (28μm) | 220 ± 27 | 6 | 6 |
| m | Distance between tips of the medial-most aesthetascs in the rows on a segment (28μm) | 196 ± 44 | 6 | 3 |
| n | Distance between tips of the lateral-most aesthetascs in the rows on a segment (28μm) | 53 ± 10 | 6 | 3 |
| o | Acute angle formed by tip of distal aesthetasc row and longitudinal axis of antennule (°) | 70 ± 5 | 6 | 3 |
| p | Obtuse angle formed by tips of proximal aesthetasc row and longitudinal axis of antennule (°) | 107 ± 8 | 6 | 3 |
| q | Acute angle formed by tips of distal and tips of proximal aesthetasc rows[b] (°) | 39 ± 8 | 6 | 6 |
| r | Angle between lateral-most aesthetasc in the distal row and antennule (°) | 48 ± 5 | 6 | 3 |
| s | Angle between lateral-most aesthetasc in the proximal row and antennule (°) | 55 ± 9 | 6 | 3 |
| t | Angle between medial-most aesthetasc in the distal row and antennule (°) | 54 ± 6 | 6 | 3 |
| u | Angle between medial-most aesthetasc in the proximal row and antennule (°) | 50 ± 6 | 6 | 3 |
| v | Angle ventrolaterally of tuft with respect to the flow during downstroke (°) | 32 ± 4 | 3 | 1 |

Values are means of the mean values from *s* measures of *n* individuals. Codes refer to Figures 1 and 2.

[a]No significant difference was found between proximal and distal rows of aesthetascs (Wilcoxon signed ranks test, $P > 0.05$), thus the results reported are pooled.

[b]No significant difference was found between angles formed by rows on same segment and those formed by rows on adjacent segments

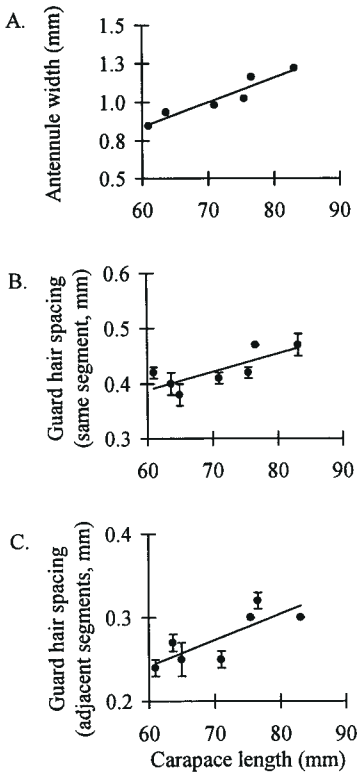


**Figure 3** Morphological parameters that varied significantly with body size plotted as a function of carapace length. **(A)** Antennule width (linear regression $y = 0.016x - 0.13$, $r^2 = 0.90$, $P = 0.004$). **(B)** Distance between guard hairs on the same segment of the antennule ($y = 0.003x + 0.19$, $r^2 = 0.60$, $P = 0.04$). **(C)** Distance between guard hairs on adjacent segments ($y = 0.003x + 0.06$, $r^2 = 0.65$, $P = 0.03$). Each symbol in (B) and (C) represents the mean value of all the measurements (error bars = 1 SD, $n = 3$) of that parameter made for an individual lobster, while in (A) only one measurement per animal is reported.

### Kinematics of a flick

The time course of the downward flick and the following upstroke are shown in Figure 4. Lobsters occasionally flicked downwards several times without intervening upstrokes; in these cases one long upstroke usually followed the series of downward flicks. During the more typical single flicks the downstroke generally lasted 0.15–0.20 s, while the upstroke was more variable in duration (0.20–0.90 s). The speed of the downstroke was much faster than that of the upstroke (Table 2). While Gleeson *et al.* estimated antennule velocity (by dividing excursion distance by flick duration) to be 0.077 m/s (Gleeson *et al.*, 1993), the temporal resolution of our high speed videos of 0.004 s permitted us to resolve that downstroke velocities peaked at 0.09 m/s while upstroke velocities were only 0.02 m/s. Our high speed video also revealed that antennule bending and whiplashing during the flick caused the mid-point of the hair-bearing region of the lateral flagellum to slow before the flagellum tip at the end of the downstroke (Figure 4A,C). The lateral flagella of the antennules bent as they moved through the water such that their instantaneous angles of attack varied with time (Figure 4B–D). Nonetheless, the mean angle of attack of the lateral flagellum during both the downstroke and the upstroke was 90° and

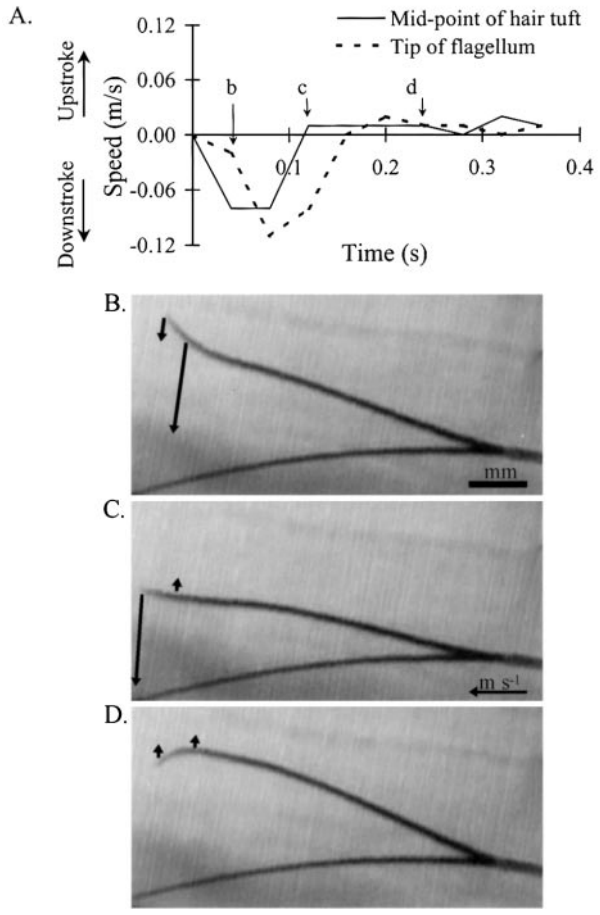


**Figure 4** Example of the kinematics of a flick by the lateral flagellum of the antennule of *P. argus*. **(A)** Graph of the speed of the tip (dashed line) and the mid-point of the tuft of hairs (solid line) of a flicking antennule as a function of time. The downstroke speeds are indicated by negative values and the upstroke speeds by positive values. **(B)** Frame of a high speed video of an antennule at the stage during its flick that corresponds to stage b indicated on the graph in (A). Arrows indicate the velocity of motion of the lateral flagellum of the antennule at its tip and at the mid-point of the tuft of hairs. Size scale bar 10 mm; velocity scale shown in (C). **(C)** Frame of a high speed video of an antennule at the stage in its flick that corresponds to c indicated on the graph in (A). Velocity scale bar 0.05 m/s; size scale shown in (B). **(D)** Frame of a high speed video of the antennule at the stage during its flick that corresponds to d indicated on the graph in (A). Size scale shown in (B); velocity scale shown in (C). Each image in (B)–(D) represents a 0.004 s interval.

the angle of attack at the time of maximum velocity during the downstroke was 90° (Table 2).

The speeds (Figure 5A) and angles of attack (Figure 5B) of the lateral flagella during flick downstrokes and upstrokes did not vary significantly with carapace length across the size range of animals studied (linear regression, $P > 0.05$ in all cases).

### Reynolds numbers of aesthetascs during flicking

The Reynolds numbers (Re = $LU\rho/\mu$) of the aesthetascs during the flick downstrokes and upstrokes were calculated for each lobster. We determined the Re of the aesthetascs for each lobster using three different speeds ($U$): the mean speed of the flick downstroke phase, the mean maximum speed attained during the downstroke and the mean upstroke speed (Table 2, Figure 5C). The downstroke Re was significantly greater than the upstroke Re (Mann–Whitney $U$-test, $P = 0.008$). Furthermore, the Re values of the downstrokes were always ≥1, while the Re values of the upstrokes were always < 1.

**Table 2** Kinematic parameters of the flick downstroke and upstroke of the lateral flagellum of the antennule of the lobster, *P. argus*

| Kinematic parameter | Mean ± SD |
|---|---|
| Angle of attack of lateral flagellum (°) | |
| Mean at maximum downstroke speed | 90 ± 4 |
| Mean during downstroke | 90 ± 10 |
| Mean during upstroke | 90 ± 10 |
| Speed (m/s) | |
| Maximum during downstroke | 0.09 ± 0.01 |
| Mean during downstroke | 0.06 ± 0.01 |
| Mean during upstroke | 0.02 ± 0.01 |
| Aesthetasc Re (calculated from the following speeds) | |
| Mean maximum speed during downstroke | 2 ± 0.4 |
| Mean speed during downstroke | 1 ± 0.5 |
| Mean speed during upstroke | 0.5 ± 0.3 |

A mean velocity was calculated for each flick downstroke and upstroke and the maximum speed attained during a downstroke was recorded. The mean values from 15 flicks per individual were calculated for these three speeds. These means were used to calculate the mean values reported for five individuals.

Since aesthetasc dimensions and speeds did not vary with body size over the range we studied, the Re values of these sensory hairs did not vary significantly with carapace length (Figure 5C) (linear regression, $P > 0.05$ in all cases).

### Temporal and spatial pattern of flicking

Examples of the antennule flicking patterns of *P. argus* are given in Figure 6. The lobsters typically flicked the lateral flagellum of an antennule several times in a row and then paused for a few seconds before executing another series of flicks. Usually the tip of the antennule was moved a distance of several centimeters vertically and/or laterally to a new location during the pause, hence successive series of flicks sampled different positions in the water. Analysis of high speed videos revealed that within a series of flicks at one position the antennule was usually held stationary for a brief interval between successive flicks (mean of the mean interval duration = 0.54 ± 0.37 s, $n = 6$ lobsters; 12–25 pauses per lobster were measured).

Antennule velocities during the repositioning that occurred between series of flicks were estimated from standard videos of undisturbed lobsters. Because the lobsters were moving about freely in a large aquarium with rocks and

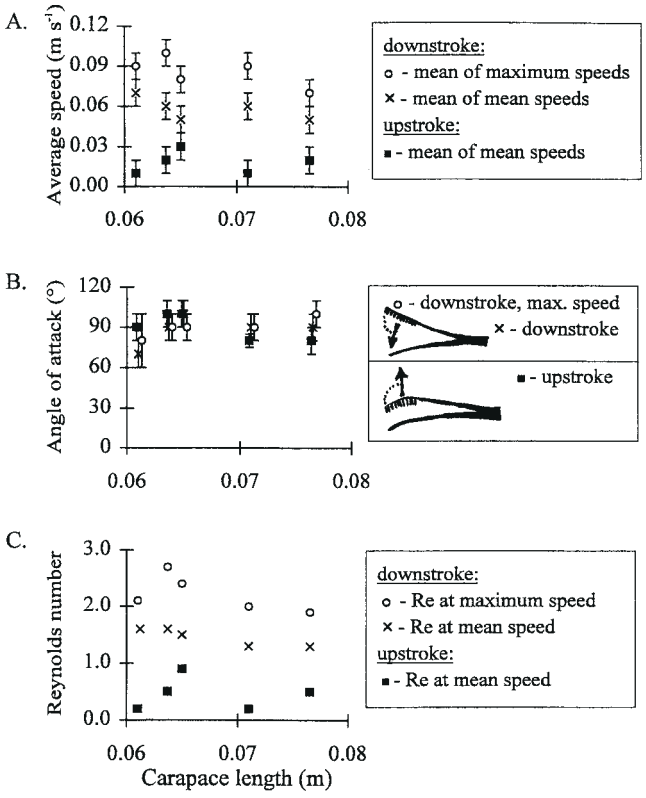


**Figure 5** Kinematic parameters plotted as a function of carapace length. Each symbol represents the mean value of 15 digitized flicks per individual, and the value for each of those flicks represents the mean of the measurements made for the frames digitized for that flick (the number of frames digitized varied depending on the duration of the flick). Error bars in (A) and (B) represent ±1 SD. **(A)** Speed of antennule measured at the mid-point of the tuft of hairs: ○, maximum speed attained during a downstroke; ×, mean speed during an entire downstroke; ■, mean speed during an entire upstroke. **(B)** Angle of attack of lateral flagellum (angle between the long axis of the lateral flagellum at the mid-point of the tuft of hairs and the velocity vector of water motion relative to the flagellum, as indicated by the dotted angles on the diagram): ○, angle at the time of maximum downstroke speed; ×, mean angle during an entire downstroke; ■, mean angle during an entire upstroke. **(C)** Re of aesthetascs: ○, Re calculated using the mean of the maximum speed attained during a downstroke; ×, Re calculated using the mean of the mean speeds during entire downstrokes; ■, Re calculated using the mean of the mean speeds during entire upstrokes.

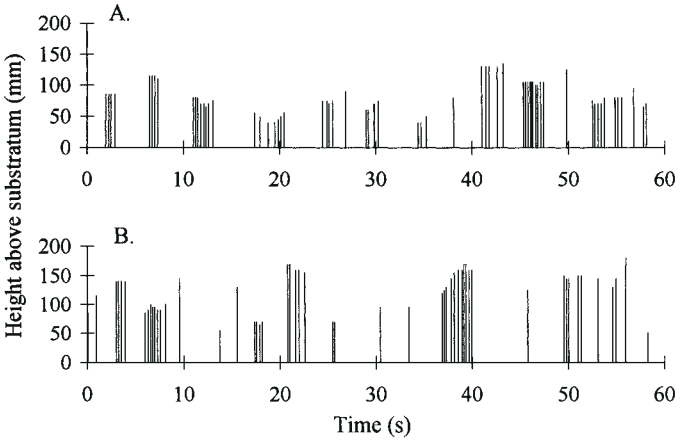


**Figure 6** Examples of the temporal and spatial patterns of antennule flicking by *P. argus*. Each flick is represented by a line that intersects the time axis at the instant (to the nearest 0.033 s) that the flick began. The height of each line represents the height above the substratum of the tip of the lateral flagellum of the antennule at the onset of each flick. **(A)** Antennule flicking by an undisturbed lobster standing still in a 246 l aquarium to which no food (shrimp) had been added during the previous 24 h. **(B)** Antennule flicking by the same lobster eating a shrimp. A dead shrimp was dropped into the aquarium 60 s after the flicking sequence in (A) was recorded and the lobster locomoted quickly and seized the prey. The sequence in (B) was recorded ~360 s later, after the lobster settled down in one spot and was eating the shrimp.

flower pots, only some video sequences provided images of antennules in full view, good focus and proper orientation to permit digitizing. Furthermore, since lateral antennule motions did not always occur in the plane of the video, their analysis would have sometimes yielded underestimates of velocity. Therefore, we only measured the vertical velocities during repositioning of antennules for comparison with vertical velocities during flicking. Mean antennule vertical speed during repositioning was 0.012 ± 0.007 m/s ($n$ = 13) for one lobster and 0.054 ± 0.039 m/s ($n$ = 14) for another, yielding a mean aesthetasc Re of 0.77 ± 0.70 ($n$ = 2). Thus, the aesthetascs of these two lobsters operated at lower Re values during repositioning than they did during flick downstrokes, but at similar Re values to those during flick upstrokes.

Average flicking frequencies were quite variable, both within and between individuals. The frequencies we measured for undisturbed lobsters ($n$ = 4) ranged between ~25 and ~90 flicks/min (0.4–1.5 Hz). When shrimp were dropped into the aquarium the lobsters began to locomote so rapidly that it was impossible to digitize their antennule motions. However, in one such instance we were able to count 59 flicks in 17 s (3.5 Hz) by a lobster that had been flicking at a rate of 87 flicks/min (1.4 Hz) prior to introduction of the shrimp. Flicking frequencies (0.6 Hz) of undisturbed lobsters calculated from data presented by Gleeson *et al.* (Gleeson *et al.*, 1993) are consistent with our measurements. Gleeson *et al.* also noted an increase in flicking frequency when food scent was introduced (Gleeson *et al.*, 1993). In one case we were able digitize antennule flicking by an animal that had settled down to eat its shrimp (Figure 6B); we found that the flicking behavior was similar to that prior to food introduction (Figure 6A), although the range of vertical heights to which an antennule was repositioned between series of flicks was greater when the lobster was eating.

## Discussion

### Flicking behavior of *P. argus*

Our high speed kinematic analysis of spiny lobsters, *P. argus*, showed that when they flick their olfactory organs

(the lateral flagella of their antennules) the sensory hairs (aesthetascs) on these structures operate at Re values of ~2 during the rapid downstroke, but at Re values of ~0.5 during the slower upstroke. A spiny lobster samples different locations in the water by executing a series of such flicks in rapid succession at one position and then moving the antennule to a different spot where it performs another series of rapid flicks. During the brief pauses between flicks within a series at one position the antennules remain stationary, but during the repositioning that occurs between series of flicks the aesthetascs encounter flow at Re values of ~0.8.

### *Panulirus argus* aesthetascs operate in a critical Reynolds number range

The aesthetascs of *P. argus* operate in the Re range of order 1. Both mathematical and physical models of fluid flow through rows of finite width cylinders have shown that small changes in velocity can cause large changes in leakiness for closely spaced hairs operating in this Re range [reviewed by Koehl (Koehl, 1995, 2000a)]. We tested this prediction for the specific morphology (see Figure 1, Table 1) of the lateral flagellum of the antennule of *P. argus* by measuring the fluid flow around a dynamically scaled physical model of the flagellum operating at the same orientations and Re values (see Tables 1, 2) used by *P. argus* antennules during the flick downstrokes and upstrokes. These experiments showed that fluid clearly moves through the array of aesthetascs during the leaky downstroke, but flows around the array during the non-leaky upstroke (Koehl, 2000a). Therefore, even though the lateral filament of an antennule executes a reciprocal motion in which it ends up where it started before the flick, its aesthetascs do not end up surrounded by the same patch of water in which they started. The 'old' water is flushed out during the leaky downstroke and is not picked up again during the less leaky upstroke.

Because the aesthetascs of *P. argus* antennules operate at a range of Re values of order 1 (in which the leakiness of the array of aesthetascs is especially sensitive to changes in velocity), the ratio of the volume of fluid flowing between the aesthetascs during the rapid flick downstroke to that during the slower upstroke or antennal repositioning movement should be greater than if the aesthetascs operated within a range of Re values an order of magnitude lower or higher [reviewed by Koehl (Koehl, 1995, 2000a)]. Thus, because the *P. argus* antennules operate in this critical range of aesthetasc Re values in which their leakiness is sensitive to speed, their ability to take discrete water samples with each flick (akin to sniffing) should be enhanced.

### Effects of ambient water currents on leakiness of arrays of aesthetascs

It is likely that *P. argus* usually encounter slow water movement in nature. *Panulirus argus* live in dens in rock or coral outcrops and in aggregations of sponges or soft corals associated with reefs (Kanciruk, 1980). Water flow within such microhabitats on coral reefs (Koehl, 1977b; Koehl and Hadfield, 1999) and on rocky shores (Koehl, 1977a, 1982, 2000b) is much slower than free stream ambient flow at a site. Furthermore, if lobsters venture out onto flat substrata away from such flow-slowing topography, they are likely to encounter velocities that are lower than free stream in the benthic boundary layer (Nowell and Jumars, 1984) of more slowly moving fluid along the substratum, as has been measured over sand flats near a coral reef (M. Koehl and T. Cooper, unpublished data). Nonetheless, because *P. argus* antennules operate in a Re range in which changes in water velocity relative to an antennule affect leakiness, we should consider whether ambient water currents influence the flow between aesthetascs.

We have made high speed (250 frames/s) close-up (field image = 3.62 × 3.16 cm) videos of *P. argus* antennules flicking in a turbulent plume of fluorescent dye in a 0.10 m/s current in a flume and used planar laser-induced fluorescence to quantify dye concentrations encountered by aesthetasc arrays on the antennules. These measurements showed that even in turbulent ambient water currents dye does not penetrate into the array of aesthetascs except during the flick downstroke (M. Koehl, J. Koseff, T. Cooper, J. Crimaldi, M. McCay and M. Wiley, unpublished data). This difference between the leakiness produced by a flick downstroke and by an ambient current of similar speed is due to the direction of the flow relative to the antennule: flow due to the flick is at right angles to the antennule, whereas flow due to ambient currents when an animal is moving upstream (as lobsters do when tracking an odor plume) is along the length of the antennule.

Since increases in velocity can lead to increases in leakiness in the Re range in which *P. argus* aesthetascs operate, we predict that the leakiness of the aesthetasc array on an antennule at right angles to ambient water flow of order 0.10 m/s or faster would be enhanced. Although we have not observed *P. argus* antennules in that orientation in rapidly flowing water, the effects of ambient currents on the flicking behavior of other crustaceans have been studied. For example, like *P. argus*, stomatopods and crabs flick their olfactory antennules in an aesthetasc Re range in which the leakiness of the array of aesthetascs is especially sensitive to changes in velocity (Koehl, 2000a). Videos of the stomatopod *Hemisquilla ensiguera* in ambient currents of 0.10 m/s in the field and in a flume showed that they changed the velocity of their flicking in a way that maintained the ratio of the Re of the fast stroke of the flick to the Re of the slow stroke of the flick (the Re of the aesthetascs was calculated using the net flow relative to the antennule due both to the ambient current and to flicking of the antennule) (K.S. Mead, personal communication). Another species of stomatopod, *Gonodactylaceus mutatus*, flicked less frequently when exposed to currents >0.10 m/s in a flume (K.S. Mead, personal communication). Blue crabs (*Callinectes sapidus*) in a flume oriented their antennules to face upstream when

flicking in ambient currents; they ceased flicking and simply held their antennules with the aesthetascs facing into the flow when ambient currents exceeded the speed of their flick downstroke (M. Martinez, M. Koehl and U. Lee, unpublished data). The latter behavior is reminiscent of the cessation of active beating of the setulose suspension feeding appendages of porcelain crabs (Trager and Genin, 1993) and barnacles (Trager *et al.*, 1990) once ambient currents exceed some threshold velocity. Thus, although it is likely that *P. argus* usually experience very slowly moving water, future studies should quantify water flow encountered by these lobsters in the field and should explore antennule orientation, flicking kinematics and olfactory searching behavior of *P. argus* exposed to different types of ambient water flow conditions.

### Comparison of antennule flicking by *Panulirus* and *Homarus*

Like *P. argus*, the clawed lobster, *H. americanus*, has served as a system for studying the neurobiology of olfactory organs (Bayer *et al.*, 1980; Borroni and Atema, 1988; Derby and Atema, 1988; Voigt and Atema, 1990; Atema and Voigt, 1995; Gomez and Atema, 1996). There are some intriguing contrasts and similarities between the antennule designs and motions of these two species.

The manner in which *H. americanus* and *P. argus* spatially sample the water around them is not the same. The excursion distance of a *H. americanus* flick [~14–15 mm, calculated from downstroke velocity and duration data reported by Moore *et al.* (Moore *et al.*, 1991)] is roughly twice that of a *P. argus* flick [~6 mm (this study) or ~9 mm (Gleeson *et al.*, 1993)], hence, *H. americanus* sweep across larger parcels of water per flick than do *P. argus*. However, *P. argus* move the tips of their very long antennules to different positions between series of flicks, whereas *H. americanus* flick their relatively short antennules in a more spatially restricted domain.

Several parallels between the antennule flicking of clawed and spiny lobsters can be noted. Both *H. americanus* (Moore *et al.*, 1991) and *P. argus* flick the lateral, but not the medial, flagellum of the antennule. Although actual velocities were not reported, *H. americanus* has been described as having a flick downstroke that is faster than the upstroke (Berg *et al.*, 1992), as we measured for *P. argus*. *Homarus americanus* can flick up to 4 Hz when 'excited' (Berg *et al.*, 1992), similar to our *P. argus* that flicked at 3.5 Hz when food was introduced into the aquarium.

Perhaps the most important similarity between the flicking of *P. argus* and *H. americanus* is that their aesthetascs operate in the same Re range. Re values we calculated for *H. americanus* using published aesthetasc diameter (30 μm) (Moore *et al.*, 1991) and antennule flicking velocities (0.12–0.15 m/s) (Moore *et al.*, 1991; Atema, 1995) are 3–4, comparable with those Best has measured for that species (B. Best, personal communication) and to those we measured for the downstroke in *P. argus*. Furthermore, as mentioned above, both species maintain this aesthetasc Re across a range of body sizes.

Clawed and spiny lobsters appear to use different mechanisms to enhance water motion between aesthetascs during flick downstrokes and to resist it during return strokes and between-flick intervals, but both of the mechanisms that they use to enhance this pulsatile sampling of odorants in their environments are especially effective at Re values of order 1, which is the Re range of their aesthetascs. The aesthetascs of *H. americanus* are arranged in rows at right angles to the long axis of the antennule, like bristles on a toothbrush [see figure 3 in Atema (Atema, 1985)] that face directly into the flow during a flick downstroke (Moore *et al.*, 1991) (P.A. Moore, personal communication). *Homarus americanus* aesthetascs splay apart during the downstroke and back together during the upstroke (Moore *et al.*, 1991). They operate in a Re range in which changes in the gap width between closely spaced hairs can produce very large changes in leakiness (Cheer and Koehl, 1987a; Koehl, 1995, 1996, 2000a), hence, such aesthetasc splaying could lead to a substantial increase in flow between the hairs during the flick downstroke. However, when the hairs move back closer together, water trapped between them should be less likely to be flushed away by ambient currents. Such aesthetasc splaying has also been observed during the flick downstrokes of the antennules of brachyuran crabs, whose aesthetascs also operate at Re values near 1 (Koehl, 2000a), and of hermit crabs (Snow, 1973).

In contrast, the aesthetascs of *P. argus* do not splay apart during a flick (Gleeson *et al.*, 1993) (this study). Another difference between *P. argus* and *H. americanus* is the arrangement and orientation of the aesthetascs on the lateral flagellum of the antennule. The rows of aesthetascs on *P. argus* antennules are bent into a zig-zag row along the antennule and this row is oriented at 32° (this study) to 35° (Gleeson *et al.*, 1993) to the flow during a flick downstroke (Figure 2). Gleeson *et al.* proposed that this configuration and orientation of aesthetascs serves to channel water flow between these sensory hairs during a flick (Gleeson *et al.*, 1993). As described above, the velocity difference between the downstroke and return stroke causes an asymmetry in the leakiness of the aesthetasc array in the Re range in which these sensory hairs operate.

We are currently using dynamically scaled physical models of both *P. argus* and *H. americanus* antennules to study the effects on leakiness asymmetry of having the aesthetascs on the downstream side of the antennule during the return stroke and to quantify the effect of the guard hairs on fluid flow near aesthetascs.

### Role of convection and diffusion in transport of molecules to aesthetascs

The kinematic and morphometric data presented in this study will be used to model the fluid flow through arrays of

*P. argus* aesthetascs and the diffusion of odorant molecules in that flow field to the surfaces of aesthetascs, using techniques we have applied to moth antennae and stomatopod antennules (Koehl, 2000a; Loudon and Koehl, 2000) (M. Stacey, K. Mead and M. Koehl, unpublished data). Although such modeling is necessary to quantify the onset slope, peak and duration of odorant concentrations arriving at the chemosensory neurons, we can use the results of the present study to assess the roles of water flow and of molecular diffusion in transporting odorant molecules to the aesthetascs.

Péclet number characterizes the importance of convection (i.e. fluid motion) relative to molecular diffusion for a particular mass transfer situation (Murray, 1977; Futrelle, 1984). Péclet number (Pé) is given by

$$\text{Pé} = LU_\infty/D$$

where $L$ is a length scale such as hair diameter, $U_\infty$ is free stream fluid velocity relative to the hair and $D$ is the diffusion coefficient of the molecule of interest in the fluid. The higher the Pé, the more important is water flow relative to molecular diffusion in getting odorants to the surface of an olfactory hair.

We calculated the Pé values of *P. argus* aesthetascs, where $L$ is mean aesthetasc diameter ($2.2 \times 10^{-5}$ m, Table 1), $D$ is the diffusion coefficient of a small molecule in water at 25°C [of order $10^{-9}$ m$^2$/s (Berg, 1983)] and $U_\infty$ is the water speed encountered by an aesthetasc in an array. We approximated $U_\infty$ as the maximum water velocity attained midway between adjacent aesthetascs; at a Re of 0.5 for arrays having a gap-to-diameter ratio of 1 this velocity is ~20% of the speed at which the array is moving (Cheer and Koehl, 1987a), whereas at Re ≥1 this velocity is about the same magnitude as the speed of the array [Abdullah and Cheer, unpublished calculations cited in Koehl (Koehl, 1992)]. Using these model results and our measurements of antennule velocities to calculate rough approximations of $U_\infty$ values, we estimated that Pé during a flick downstroke is ~1300, while during an upstroke and during repositioning Pé is ~100–200. Pé values so much greater than 1 indicate that during both phases of the flick and during repositioning convection rather than diffusion is the mechanism bringing odorants near aesthetascs. In contrast, during the brief intervals between the flicks in a series at one position, when the antennule is held stationary, Pé is essentially zero and molecular diffusion is the mechanism bringing odorant molecules near the surfaces of the aesthetascs. Although these inter-flick intervals are only ~0.54 s, there is ample time for odorant molecules in the water trapped between the aesthetascs to diffuse to the surfaces of the aesthetascs: the root mean square displacement of molecules by diffusion in such a time interval is 33 μm [root mean square displacement = $(2Dt)^{0.5}$, where $D$ is the diffusion coefficient and $t$ is the time interval (Berg, 1983)], greater than the half-gap width between adjacent aesthetascs (Figure 1).

### Design of hair-bearing olfactory antennules

The odor-capturing antennules of malacostracan crustaceans, such as lobsters, stomatopods and crabs, bear arrays of hair-like chemosensory aesthetascs. It has been hypothesized that crustacean antennule flicking is functionally like mammalian sniffing: during the flick 'old' fluid trapped between the aesthetascs is washed away and replaced by 'new' fluid (Snow, 1973; Schmidt and Ache, 1979; Atema, 1985; Gleeson *et al.*, 1993), resulting in a pulsatile (Atema, 1985) sampling of odors in the environment. The antennules of *P. argus* (this study) and a variety of other crustaceans (Mead *et al.*, 1999; Koehl, 2000a) operate over a range of aesthetasc spacings and Re values at which their leakiness is especially sensitive to changes in velocity or in the gap-to-diameter ratio of the aesthetascs. Therefore, by altering the velocity or by changing the aesthetasc spacing between the flick downstroke and return stroke, the antennules can take discrete samples of water and can change the flux of molecules to the surfaces of their chemosensory aesthetascs. Thus, by operating in this critical Re range, these antennules should be particularly effective at sniffing.

## Acknowledgements

We are grateful to B. Ache and R. Gleeson for generously providing us with lobsters and antennules, as well as with the inspiration for this work. We thank R. Full for the use of his high speed video system, R. Kram for assistance with high speed videotaping, D. Davis for instruction in the use of facilities in the Biological Sciences Electron Microscope Laboratory at University of California–Berkeley, the Duke University Morphometrics Laboratory for use of video and graphics equipment, M. O'Donnell for help with manuscript preparation and S. Vogel for critical reading of a draft of this paper. This research was supported by Office of Naval Research grants 14-98-0775, N00014-96-1-0594 and N00014-98-0775 to M.K.

## References

**Alexander, R.McN.** (1971) Size and Shape. Edward Arnold, London.

**Ache, B.W.** (1982) *Chemoreception and thermoreception*. In Atwood, H.L. and Standeman, D.C. (eds), The Biology of the Crustacea, Vol. 3. Academic Press, New York, pp. 369–393.

**Ache, B.W.** (1988) *Integration of chemosensory information in aquatic invertebrates*. In Atema, J., Fay, R.R., Popper, A.N. and Tavolga, W.N. (eds), Sensory Biology of Aquatic Animals. Springer-Verlag. New York, pp. 387–401.

**Anderson, P.A.V.** and **Ache, B.W.** (1985) *Voltage and current clamp recordings of the receptor potential in olfactory cells* in situ. Brain Res., 338, 273–280.

**Atema, J.** (1977) *Functional separation of smell and taste in fish and crustacea*. In LeMagnen. J. and MacLeod, L. (eds), Olfaction and Taste IV. Information Retrieval, London, UK, pp. 165–174.

**Atema, J.** (1985) *Chemoreception in the sea: adaptations of chemo-*

*receptors and behavior to aquatic stimulus conditions*. Soc. Exp. Biol. Symp., 39, 387–423.

**Atema, J.** (1995) *Chemical signals in the marine environment: dispersal, detection, and temporal signal analysis*. In Eisner, T. and Meinwals, J. (eds), Chemical Ecology: The Chemistry of Biotic Interactions. National Academy Press, Washington, DC, pp. 147–159.

**Atema, J.** (1996) *Eddy chemotaxis and odor landscapes: exploration of nature with animal sensors*. Biol. Bull., 191, 129–138.

**Atema, J.** and **Voigt, R.** (1995) *Behavior and sensory biology*. In Factor, I.R. (ed.), Biology of the Lobster *Homarus americanus*. Academic Press, New York, pp. 313–348.

**Bayer, T.A., McClintock, T.S., Grunert, U.** and **Ache, B.W.** (1980) *Histamine-induced modulation of olfactory receptor neurons in two species of lobsters,* Panulirus argus *and* Homarus americanus. J. Exp. Biol., 145, 133–146.

**Berg, H.C.** (1983) Random Walks in Biology. Princeton University Press, Princeton, NJ.

**Berg, K., Voigt, R.** and **Atema, J.** (1992) *Flicking in the lobster* Homarus americanus*: recordings from electrodes implanted in antennular segments*. Biol. Bull., 183, 377–378.

**Borroni, P.F.** and **Atema, J.** (1988) *Adaptation in chemoreceptor cells I. Self-adapting backgrounds determine threshold and cause parallel shift of response function*. J. Comp. Physiol., 164A, 67–74.

**Cheer, A.Y.L.** and **Koehl, M.A.R.** (1987a) *Paddles and rakes: fluid flow through bristled appendages of small organisms*. J. Theor. Biol., 129, 185–199.

**Cheer, A.Y.L.** and **Koehl, M.A.R.** (1987b) *Fluid flow through filtering appendages of insects*. IMA J. Math. Appl. Med. Biol., 4, 185–199.

**Davies, C.N.** (1973) Air Filtration. Academic Press, New York.

**Derby, C.D.** and **Atema, J.** (1988) *Chemoreceptor cells in aquatic invertebrates: peripheral mechanisms of chemical signal processing in decapod crustaceans*. In Atema, J., Fay, R.R., Popper, A.N. and Tavolga, W.N. (eds), Sensory Biology of Aquatic Animals. Springer-Verlag, New York, pp. 365–386.

**DeSimone, J.A.** (1981) *Physicochemical principles in taste and olfaction*. In Cagan, R.H. and Kare, M.R. (eds), Biochemistry of Taste and Olfaction. Academic Press, New York, pp. 213–229.

**Fuchs, N.A.** (1964) The Mechanics of Aerosols. Oxford University Press, Oxford, UK.

**Futrelle, R.P.** (1984) *How molecules get to their detectors: the physics of diffusion of insect pheromones*. Trends. Neurosci., April, 116–120.

**Fuzessery, Z.M., Carr, W.F.S.** and **Ache, B.W.** (1978) *Antennular chemosensitivity in the spiny lobster,* Panulirus argus*: studies of taurine sensitivity receptors*. Biol. Bull., 154, 226–240.

**Gleeson, R.A.** (1982) *Morphological and behavioral identification of the sensory structures mediating pheromone reception in the blue crab,* Callinectes sapidus. Biol. Bull., 163, 162–171.

**Gleeson, R.A., Carr, W.E.S.** and **Trapido-Rosenthal, H.G.** (1993) *Morphological characteristics facilitating stimulus access and removal in the olfactory organ of the spiny lobster,* Panulirus argus*: insight from the design*. Chem. Senses, 18, 67–75.

**Gomez, G.** and **Atema, J.** (1996) *Temporal resolution in olfaction: stimulus integration time of lobster chemoreceptor cells*. J. Exp. Biol., 199, 1771–1779.

**Grunert, U.** and **Ache, B.W.** (1988) *Ultrastructure of the aesthetasc (olfactory) sensilla of the spiny lobster* Panulirus argus. Cell Tissue Res., 251, 95–103.

**Hallberg, E., Johansson, K.U.I.** and **Elofsson, R.** (1992) *The aesthetasc concept: structural variations of putative olfactory receptor cell complexes in crustaceans*. Microsc. Res. Technol., 22, 336–350.

**Hansen, B.** and **Tiselius, P.** (1992) *Flow through the feeding structures of suspension feeding zooplankton: a physical model approach*. J. Plankton Res., 14, 821–834.

**Happel, J.** and **Brenner, H.** (1965) Low Reynolds Number Hydrodynamics with Special Applications to Particulate Media. Prentice-Hall, Englewood Cliffs, NJ.

**Kanciruk, P.** (1980) *Ecology of juvenile and adult Palinuridae (spiny lobsters)*. In Cobb, J.S. and Philips, B.F. (eds), The Biology and Management of Lobsters, Vol II. Ecology and Management. Academic Press, New York, pp. 59–96.

**Koehl, M.A.R.** (1977a) *Effects of sea anemones on the flow forces they encounter*. J. Exp. Biol., 69, 87–105.

**Koehl, M.A.R.** (1977b) *Water flow and the morphology of zoanthid colonies*. In Taylor, D.L. (ed.), Proceedings of the Third International Coral Reef Symposium, Vol. 1. Rosensteil School of Marine and Atmospheric Science, University of Miami, Miami, FL, pp. 437–444.

**Koehl, M.A.R.** (1982) *The interaction of moving water and sessile organisms*. Scient. Am., 247, 124–132.

**Koehl, M.A.R.** (1992) *Hairy little legs: feeding, smelling, and swimming at low Reynolds number*. Contemp. Math., 141, 33–64.

**Koehl, M.A.R.** (1995) *Fluid flow through hair-bearing appendages: feeding, smelling, and swimming at low and intermediate Reynolds number*. Soc. Exp. Biol. Symp., 49, 157–182.

**Koehl, M.A.R.** (1996) *Small-scale fluid dynamics of olfactory antennae*. Mar. Freshwat. Behav. Physiol., 27, 127–141.

**Koehl, M.A.R.** (2000a) *Fluid dynamics of animal appendages that capture molecules: arthropod olfactory antennae*. In Fauci, L. and Gueron, S. (eds), Computational Modeling in Biological Fluid Dynamics. IMA Volumes in Mathematics and its Applications, Vol. 124. Springer-Verlag, New York, pp. 97–116.

**Koehl, M.A.R.** (2000b) *Mechanical design and hydrodynamics of blade-like algae:* Chondracanthus exasperatus*.* In Spatz, H.C. and Speck, T. (eds), Proceedings of the Third International Plant Biomechanics Conference. Thieme Verlag, Stuttgart, Germany.

**Koehl, M.A.R.** and **Hadfield, M.** (1999) *Can larvae of benthic animals use dissolved chemical cues in wave-driven flow?* EOS, 80, OS295.

**Koehl, M.A.R.** and **Strickler, J.R.** (1981) *Copepod feeding currents: food capture at low Reynolds number*. Limnol. Oceanogr., 26, 1062–1073.

**Laverack, M.S.** (1988) *The diversity of chemoreceptors*. In Atema, J., Fay, R.R., Popper, A.N. and Tavolga, W.N. (eds), Sensory Biology of Aquatic Animals. Springer-Verlag, New York, pp. 287–317.

**Leonard, A.B.P.** (1992) The Biomechanics, Autecology and Behavior of Suspension-feeding in Crinoid Echinoderms. PhD dissertation, University of California–San Diego, San Diego, CA.

**Loudon, C.** and **Koehl, M.A.R.** (2000) *Sniffing by a silkworm moth: wing fanning enhances air penetration through and pheromone interception by antennae*. J. Exp. Biol., 203, 2977–2990.

**Loudon, C., Best, B.A.** and **Koehl, M.A.R.** (1994) *When does motion relative to neighboring surfaces alter the flow through an array of hairs?* J. Exp. Biol., 193, 233–254.

**Marschall, H.P.** and **Ache, B.W.** (1989) *Response dynamics of lobster*

*olfactory neurons during simulated natural sampling*. Chem. Senses, 14, 725.

**Marx, J.** and **Herrnkind, W.** (1985) *Factors regulating microhabitat use by young juvenile spiny lobsters,* Panulirus argus*: food and shelter*. J. Crustacean Biol., 5, 650–657.

**Mead, K.S., Koehl, M.A.R.** and **O'Donnell, M.J.** (1999) *Stomatopod sniffing: the scaling of chemosensory sensillae and flicking behavior with body size*. J. Exp. Mar. Biol. Ecol., 241, 235–261.

**Michel, W.C., McKlintock, T.S.** and **Ache, B.W.** (1991) *Inhibition of lobster olfactory receptor cells by an odor-activated potassium conductance*. J. Neurophysiol., 65, 446–453.

**Moore, P.A.** (1994) *A model of adaptation and disadaptation in olfactory receptor neurons: implications for the coding of temporal and intensity patterns in odor signals*. Chem. Senses, 19, 71–86.

**Moore, P.A.** and **Atema, J.** (1988) *A model of a temporal filter in chemoreception to extract directional information from a turbulent odor plume*. Biol. Bull., 174, 355–363.

**Moore, P.A.** and **Atema, J.** (1991) *Spatial information in the three-dimensional fine structure of an aquatic odor plume*. Biol. Bull., 181, 408–418.

**Moore, P.A., Gerhardt, G.A.** and **Atema, J.** (1989) *High resolution spatio-temporal analysis of aquatic chemical signals using microelectrochemical electrodes*. Chem. Senses, 14, 829–840.

**Moore, P.A., Atema, J.** and **Gerhardt, G.A.** (1991) *Fluid dynamics and microscale chemical movement in the chemosensory appendages of the lobster,* Homarus americanus. Chem. Senses, 16, 663–674.

**Moore, P.A., Weissburg, M.J., Parrish, J.M., Zimmer-Faust, R.K.** and **Gerhardt, G.A.** (1994) *Spatial distribution of odors in simulated benthic boundary layer flows*. J. Chem. Ecol., 20, 255–279.

**Murlis, J.** (1986) *The structure of odour plumes*. In Payne, T.L., Birch, M.C. and Kennedy, C.E.J. (eds), Mechanisms of Insect Olfaction. Clarendon Press, Oxford, UK, pp. 27–38.

**Murray, J.D.** (1977) *Reduction of dimensionability in diffusion processes: antenna receptors of moths*. In Murray, J.D. (ed.), Lectures on Nonlinear-Differential-Equation Models in Biology. Oxford University Press, Oxford, UK, pp. 83–127.

**Nowell, A.R.M.** and **Jumars, P.A.** (1984) *Flow environments of aquatic benthos*. Annu. Rev. Ecol. Syst., 15, 303–328.

**Ratchford, S.G.** and **Eggleston, D.B.** (1998) *Temporal shift in the presence of a chemical cue contributes to a diel shift in sociality*. Anim. Behav., 59, 793–799.

**Rubenstein, D.I.** and **Koehl, M.A.R.** (1977) *The mechanisms of filter feeding: some theoretical considerations*. Am. Naturalist, 26, 981–994.

**Schmidt, B.C.** and **Ache, B.W.** (1979) *Olfaction: responses of a decapod crustacean are enhanced by flicking*. Science, 205, 204–206.

**Shimeta, J.** and **Jumars, P.A.** (1991) *Physical mechanisms and rates of particle capture by suspension-feeders*. Oceanogr. Mar. Biol. Annu. Rev., 29, 191–257.

**Snow, P.J.** (1973) *The antennular activities of the hermit crab,* Pagarus alaskensis *(Benedict)*. J. Exp. Biol., 58, 745–765.

**Sverdrup, H.U., Johnson, M.W.** and **Fleming, R.H.** (1942) The Oceans: Their Physics, Chemistry, and General Biology. Prentice-Hall, New York.

**Trager, G.** and **Genin, A.** (1993) *Flow velocity induces a switch from active to passive suspension feeding in the porcelain crab* Petrolisthes leptocheles *(Heller)*. Biol. Bull., 185, 20–27.

**Trager, G.C., Hwang, J.S.** and **Strickler, J.R.** (1990) *Barnacle suspension-feeding in variable flow*. Mar. Biol., 105, 117–128.

**Vogel, S.** (1983) *How much air passes through a silkmoth's antenna?* J. Insect Physiol., 29, 597–602.

**Vogel, S.** (1994) Life in Moving Fluids: The Physical Biology of Flow, 2nd Edn. Princeton University Press, Princeton, NJ.

**Voigt, R.** and **Atema, J.** (1990) *Adaptation in chemoreceptor cells. III: Effects of cumulative adaptation*. J. Comp. Physiol., 166A, 865–874.

**Weissburg, M.J.** and **Zimmer-Faust, R.K.** (1994) *Odor plumes and how blue crabs use them in finding prey*. J. Exp. Biol., 197, 349–375.

**Willis, M.A., David, C.T., Murlis, J.** and **Carde, R.T.** (1994) *Effects of pheromone plume structure and visual stimuli on the pheromone-modulated upwind flight of male gypsy moths (*Lumantria dispar*) in a forest (Lepidoptera, Lymantriidae)*. J. Insect Behav., 7, 385–409.

**Zar, J.H.** (1974) Biostatistical Analysis. Prentice-Hall, Englewood Cliffs, NJ.

**Zerbe,W.B.** and **Taylor, C.B.** (1953) *Sea water temperature and density reduction tables*. In Coast and Geodetic Survey Special Publication no. 298. US Department of Commerce, Washington, DC, pp. 18–19.

**Zimmer-Faust, R.K., Stanfill, J.M.** and **Collard, S.B.** (1988) *A fast, multichannel fluorometer for investigating aquatic chemoreception and odor trail*. Limnol. Oceanogr., 33, 1586–1595.

*Accepted November 27, 2000*